JACS
JOURNAL OF THE AMERICAN CHEMICAL SOCIETY

Communication

pubs.acs.org/JACS

Ion-Gated Synthetic Photosystems

Naomi Sakai, Pierre Charbonnaz, Sandra Ward, and Stefan Matile*

Department of Organic Chemistry, University of Geneva, CH-1211 Geneva, Switzerland

Supporting Information

ABSTRACT: Herein, molecular strings of ions built along charge-transporting channels are shown to dramatically increase photocurrents and enable charge transport over long distances, thus confirming the existence and significance of ion-gated photosystems. For their synthesis, ordered and oriented stacks of naphthalenediimides were grown on indium tin oxide by ring-opening disulfide-exchange polymerization. To these charge-transporting channels, coaxial strings of anions or cations—fixed, mobile, complete, partial, pure, or mixed—were added by orthogonal hydrazone exchange. The presence of partially protonated carboxylates was found to most significantly increase activity, implying that they both attract holes and repel electrons, that is, facilitate photoinduced charge separation and hinder charge recombination at the same time. As a result of this quite remarkable situation, photocurrents increased rather than decreased with increasing charge stabilization on their "stepping stones." The presence of mobile anions facilitated long-distance charge transport through thick films. Turned off by inhibited anion mobility, that is, proton hopping, hole/proton antiport is identified to account for long-distance charge transport in ion-gated photosystems.

The efficient generation and transport of charges are fundamental in material sciences as well as in biology.[1] In biological systems, charges usually migrate over long distance via successive hopping from one site to another.[1a−c] These hopping sites consist of relatively easily oxidizable residues/bases, charges on which are further stabilized by simultaneous proton transfer in proton-coupled electron transfer[2] or by the reorganization of polar surrounding molecules including ions.[3] Although numerous model studies established the significance of proton-coupled electron transfer in biological charge transport, the importance of counterions attracted much less attention.[3] DNA is the privileged scaffold to study environmental effects on charge transport, and indeed, the critical importance of backbone phosphates was found for efficient electron transport over long distances.[1a,b,3a] Ions attached next to electroactive moieties are also known to influence their redox properties through charge repulsion or attraction[3c,d] and, thus, the rate of charge separation and recombination.[3e,f] We were particularly intrigued by the possibility to modulate the rate of long-distance charge transport by incorporating ion-gated redox gradients[4] in the charge-conducting pathway. Herein, we report the influence of surrounding counterions on charge transport through π-stacked organic semiconductors using photocurrent generation as a readout.

To construct desired photosystems with ionizable groups attached along charge-transporting pathways, self-organizing surface-initiated polymerization with templated stack exchange (SOSIP-TSE) was the ideal synthetic approach (Scheme 1).[5] In brief, SOSIP of propagators containing two protected hydrazides is initiated by thiolate groups in initiators that are covalently bound to a conductive indium tin oxide (ITO) surface. Molecular recognition between the propagator and the initiator on the ITO surface aligns the central aromatic units before ring-opening disulfide-exchange polymerization takes place and, thus, produces oriented π-stack architectures as shown in **1**.[6] Although the compatibility with the other aromatic units is proven,[5b,7] current studies are mostly conducted with best established electron-deficient alkoxy-substituted naphthalenediimides (NDIs) as the central charge-transporting unit.[8] Their ability to undergo symmetry-breaking charge separation and to generate photocurrent has been already demonstrated.[9,10] Mild, efficient, and tolerant to the size and nature of stack exchangers, TSE seems well suited for the controlled incorporation of ions into the photosystems. Thus, aldehydes with ionizable groups **2**−**4** were synthesized as

Scheme 1. ***a.*** **(1) NH_2OH, (2) 2, 3, or 4, AcOH, (3) Tris buffer pH 7.4**

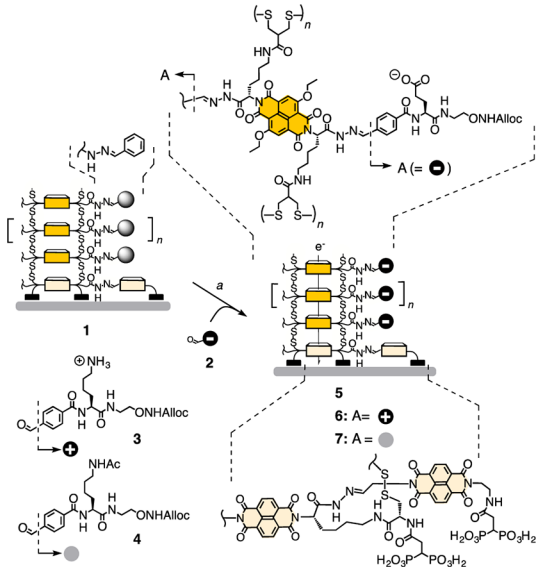

Received: February 10, 2014
Published: April 1, 2014

   dx.doi.org/10.1021/ja501389g | J. Am. Chem. Soc. 2014, 136, 5575−5578

stack exchangers from amino-acid derivatives by standard peptide synthesis methodology (Supporting Information (SI) Scheme S1). Then, starting from the already reported photosystem **1**,[5a] removal of the benzaldehyde protecting group, hydrazone bond formation with aldehyde **2** containing a glutamate residue, followed by an equilibration in neutral buffer resulted in the desired oriented π-stacked architecture **5** with negative charges attached along the conductive pathways. Interestingly, >5 h of equilibration at 40 °C was necessary to achieve stable photocurrents (see below). Control experiments with pH-sensitive NDI stacks[11] confirmed that strongly decelerated acid−base chemistry accounts for this exceptionally slow response, presumably because of hindered diffusion of buffer within the complex surface architectures (not shown). Slow acid−base chemistry has been observed before in organic materials, although not to this extent.[12] The photosystems with positive (**6**) or neutral charges (**7**) were prepared similarly using lysine or acetyl-lysine containing aldehyde **3** or **4**, respectively. According to absorption spectroscopy, hydrazone exchange reactions proceeded in high yield (>86%) in all the photosystems, and the obtained hydrazones were stable in neutral buffer at 40 °C for >3 days (SI Figure S1a). AFM images demonstrated that the highly ordered structures characteristic of SOSIP architectures[5] remain intact under these conditions (SI Figure S1c).

Photocurrent generation was examined using the photosystem as working electrode, a Pt wire as counter electrode and an Ag/AgCl reference electrode, all immersed in a buffer containing a mobile hole carrier, triethanol amine (TEOA). As expected, pH dependence of photocurrent generation demonstrated significant difference among the photosystems with different charges (SI Figure S3a). In general, photocurrent decreased upon lowering of pH because of the decreasing concentration of active neutral TEOA in this pH range. Thus, the neutral photosystem **7** was used as a reference to reveal true pH dependence of photoactivity (Figure 1b). Compared with the almost unresponsive **6**, the clearly different, bell-shaped pH dependence observed for photosystem **5** suggested that partial deprotonation promotes photocurrent generation (Figure 1b, ● vs ○). The presence of protonated and deprotonated carboxylic acids at pH ∼ 7.5 seems reasonable considering that because of intramolecular charge repulsion, complete deprotonation of polyglutamic acid occurs at pH ∼ 9, about four units above the intrinsic pK_a of the carboxylic acids.[13] Significantly higher photocurrent generation at pH ∼ 7.5 by photosystem **5** compared with **6** or **7** could then be rationalized by facilitated photoinduced charge separation between NDIs with and without anion. Namely, as nearby carboxylates raise HOMO and LUMO energy levels of NDIs by about 50 mV,[3c] charge separation between them would be energetically favorable (Figure 1c, HOMO = highest occupied molecular orbital, LUMO = lowest unoccupied molecular orbital). Moreover, the charge-separated state would be stabilized not only by the Coulombic attraction between holes and carboxylate anions but also by the repulsion between the electrons and anions.

Photosystems **5′** containing both anions and neutral groups like photosystem **5** around pH 7.5 was prepared by conducting mixed TSE with **2** and **4**. Unlike in photosystem **5** around pH 7.5, anions in this system cannot migrate together with charges. Measured at full deprotonation at pH 9, photosystem **5′** generated only about 50% more photocurrent compared to photosystem **7** (I/I_0 ∼ 1.5). This result indicated that for the generation of the large photocurrents by photosystem **5** around

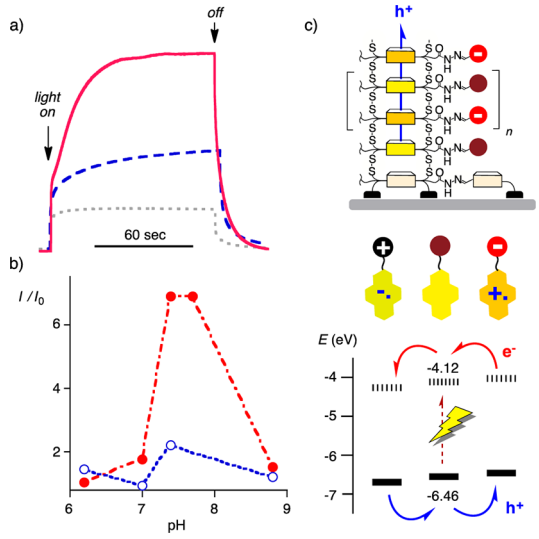

Figure 1. (a) Photocurrent I generated by anionic (**5**, red solid line), cationic (**6**, blue dashed line), and neutral photosystems (**7**, gray dotted line) in response to irradiation with a solar simulator (power, 28 mW cm^{-2}; 50 mM TEOA, 0.2 M $Na_mH_nPO_4$ buffer, pH 7.7 at 0 V vs Ag/AgCl). (b) pH dependence of photocurrent I at saturation by **5** (●) and **6** (○) relative to **7** (I_0) (irradiation with solar simulator, P = 28 mW cm^{-2}; 50 mM TEOA, 0.2 M sodium phosphate buffer, pH 6.2−8.8 at 0 V vs Ag/AgCl). (c) Anionic photosystem **5** at near neutral pH, with expected HOMO (bold) and LUMO (dashed) energy levels of NDIs with/without ions (in electronvolts against a vacuum, normalized for −5.1 eV for Fc^+/Fc).

pH 7.5 (I/I_0 ∼ 7, Figure 1b), the hole-stabilizing counterions move together with their holes by relaying protons in the other direction along the coaxial string of partially protonated carboxylic acids. Although similar mechanisms could apply to the cationic photosystem **6**, the observed much lower photocurrent suggested that in this system, the stabilization of electrons is less important than the stabilization of holes.

To gain further insight on ion gating, the temperature dependence of photocurrent generation was investigated. As implied from the biphasic kinetics (Figure 1a), photocurrent generation by the anionic photosystem **5** increased sharply as the temperature of the buffer was raised (Figure 2a, ●). The temperature dependence was much weaker with cationic or

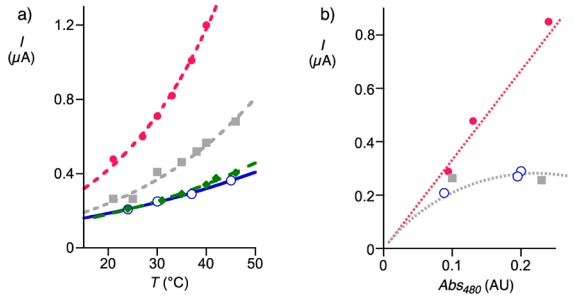

Figure 2. (a) Temperature dependence of the initial photocurrent by **5** (●), **6** (○), **7** (■), and **1** (♦) in response to irradiation with a solar simulator (power, 75 mW cm^{-2}; 50 mM TEOA, 0.2 M sodium phosphate buffer, pH 7.7 at 0 V vs Ag/AgCl at 20−46 °C) fitted to the Arrhenius equation. (b) Dependence of photocurrent generation on the thickness of films for **5** (●), **6** (○), and **7** (■). A_{480} = 0.1 corresponds roughly to 30 nm film thickness,[9] curves are added as visual guides.

dx.doi.org/10.1021/ja501389g | J. Am. Chem. Soc. 2014, 136, 5575−5578

neutral photosystems **6** and **7** (Figure 2a, ○ and ■). By applying the Arrhenius equation ($k = A\exp(-E_a/RT)$) to the photocurrent-temperature dependence, the activation energy E_a could be estimated (Figure 2a). The obtained values (i.e., E_a (**5**) = 0.40 eV > E_a (**7**) = 0.33 eV > E_a (**1**) = 0.25 eV > E_a (**6**) = 0.19 eV) were in the range of organic semiconductors,[14] DNA,[15] or peptides[16] but larger than those found with some highly conductive organic materials.[17a,18]

According to a multistep hopping mechanism, charge transport occurs via thermal activation of charge carriers residing mostly on "stepping stones" or "relays".[1,17] Highest E_a found for the anionic photosystem **5**, thus, implied that hole transport is rate limiting, which is reasonable because NDIs are well-known n-semiconductors.[8,19] The found correlation between high photocurrent and high E_a demonstrated that stabilization of the charge-separated state, and thus, deceleration of charge recombination determines photocurrent generation.[20] Consistent with the ability of "mobile" counterions to assist charge transport over long distances by moving together with the holes they stabilize and protect, only the anionic photosystem **5** generated more photocurrent when the thickness of the film was increased (Figure 2b, ● vs ○ and ■).

These results suggested that the stepwise installation of anionic and cationic groups along NDI π-stacks would result in charge-transporting pathways with redox gradients. We have previously shown that redox gradients improve the overall performance of synthetic photosystems.[4,5a,c] In those systems, we installed redox gradients using different chromophores. Here, we were interested in the possibility to build gradients by directionally attaching ions along single-component charge-transporting pathways. As in previous examples, partial removal and exchange of stack exchangers proceeded in high yield to give the desired gradient systems **8** and **9** (SI Figure S1b). However, contrary to our expectations, the photosystem **8** with a favorable redox gradient generated less photocurrent than **9** (Figure 3, ● vs ♦). The overall larger contribution of ions near the electrode surface supported the critical importance of stabilizing holes that are generated near the electrode and far from the hole acceptor in solution.

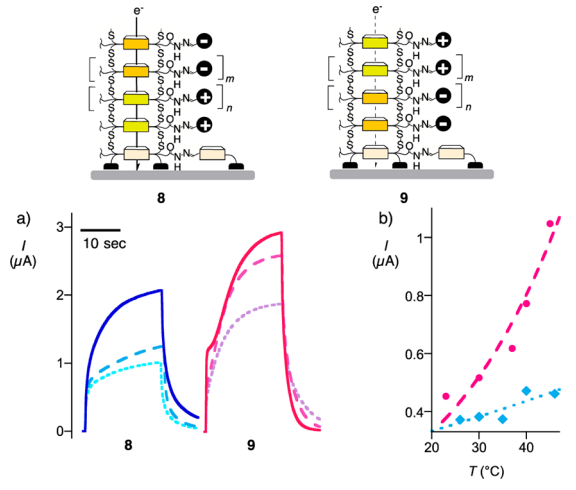

Figure 3. (a) Temperature-dependent photocurrent generation by gradient photosystems **8** and **9**. From lower to higher photocurrent, measured at about 25, 35, and 45 °C. For other conditions, see Figure 2. (b) Dependence of the initial photocurrent by photosystem **8** (♦) and **9** (●) to the temperature.

The effect of ions was further examined using unsubstituted NDI-perylenediimide (PDI) heterojunction photosystems **10**–**12** (Figure 4).[5d] Although both NDIs and PDIs are n-

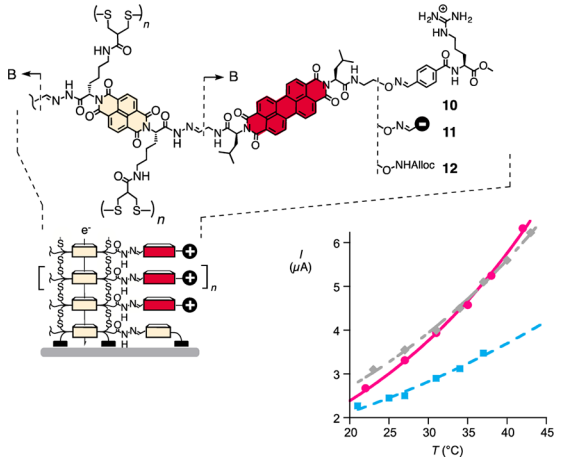

Figure 4. Structures of double-channel photosystems **10**–**12** with/without appended ions. Inset: Temperature dependence of photocurrent generation by **10** (■), **11** (●), and **12** (♦).

semiconductors, surprisingly large photocurrents generated by dyad **12** suggested efficient electron transfer from PDIs to NDIs. The ability of PDIs to act as a hole transporter has been demonstrated theoretically[21] and experimentally.[22] According to the above interpretations, ions are expected to affect systems with efficient charge separation in the same way but less significantly. Using the "triple-channel" strategy,[5d] ionic moieties were first attached to PDIs via oxime bonds. Subsequent stack exchange with the obtained conjugates gave the NDI-PDI double-channel photosystems with ions attached along the PDI channels (SI Figure S2).

In the cationic photosystem **10**, guanidinium instead of ammonium groups were used to prevent the intramolecular imine formation, which was found to hamper efficient stack exchange. Unlike in the case of single-channel photosystems, almost the same photocurrent was generated by anionic photosystem **11** and the neutral control **12** over the pH range tested (SI Figure S3). These results were in agreement with above conclusion that partial charges can facilitate symmetry-breaking charge separation between identical chromophores, but that such ion gating should become less important with efficient donor–acceptor dyads. Correspondingly weaker effects of ions were found in the temperature dependence of photocurrent generation (Figure 4). However, the observed trends for the activation energies were as with the single-channel systems **5**–**7** (Figure 2a), that is, E_a (**11**) = 0.31 eV > E_a (**12**) = 0.29 eV > E_a (**10**) = 0.20 eV (Figure 4). Although linear correlations were found between photocurrent and thickness of films with both **11** and **12**, slightly higher E_a supported the potential of anionic photosystem **11** to transport charges over longer distances (SI Figure S3).

In summary, we have shown that photocurrent generation can be greatly influenced by ions attached along the charge transporting pathways. Anions were found to improve the photocurrent generation by stabilizing holes and preventing charge recombination at the same time. Most importantly, "mobile" anions are demonstrated to mediate hole transfer over long distances by a coupled proton antiport along a coaxial string of mixed carboxylic acids and carboxylates, whereas

dx.doi.org/10.1021/ja501389g | J. Am. Chem. Soc. 2014, 136, 5575–5578

"fixed" counterions fail to do so. Depending on the nature of the charge-transporting channel, similar mechanisms will apply also to electrons and cations.

Considering that long-distance charge-transfer is a fundamental process in the materials sciences as well as in biology,[1−3,23] the lessons learned in this study should be of high general significance. They might help to better understand biological charge transfer involved in respiration, photosynthesis or enzymatic transformations (ribonucleotide reductase, photolyase, etc).[1−3,23] Conductive pilin filaments, for example, which are responsible to electronically connect bacteria with ferric oxide minerals, are composed of helix bundles with clusters of charged and aromatic amino acids.[23] Transcribed to the materials science, we hope that these results will encourage the strategic positioning of "fixed" or "mobile" counterions for the design and development of future advanced organic electronics, for example, solar cells, field-effect transistors, light emitting diodes, nanowires, and so forth.

■ ASSOCIATED CONTENT

Supporting Information

Detailed experimental procedures. This material is available free of charge via the Internet at http://pubs.acs.org.

■ AUTHOR INFORMATION

Corresponding Author

Stefan.Matile@unige.ch

Notes

The authors declare no competing financial interest.

■ ACKNOWLEDGMENTS

We thank the NMR and the Sciences Mass Spectrometry (SMS) platforms for services, and the University of Geneva, the European Research Council (ERC Advanced Investigator), the National Centre of Competence in Research (NCCR) in Chemical Biology, and the Swiss NSF for financial support.

■ REFERENCES

(1) (a) Genereux, J. C.; Barton, J. K. *Chem. Rev.* **2010**, *110*, 1642−1662. (b) Giese, B. *Acc. Chem. Res.* **2000**, *33*, 631−636. (c) Cordes, M.; Giese, B. *Chem. Soc. Rev.* **2009**, *38*, 892−901. (d) Beaujuge, P. M.; Fréchet, J. M. J. *J. Am. Chem. Soc.* **2011**, *133*, 20009−20029. (e) Morisue, M.; Yamatsu, S.; Haruta, N.; Kobuke, Y. *Chem.—Eur. J.* **2005**, *11*, 5563−5574.

(2) (a) Weinberg, D. R.; Gagliardi, C. J.; Hull, J. F.; Murphy, C. F.; Kent, C. A.; Westlake, B. C.; Paul, A.; Ess, D. H.; McCafferty, D. G.; Meyer, T. J. *Chem. Rev.* **2012**, *112*, 4016−4093. (b) Dempsey, J. L.; Winkler, J. R.; Gray, H. B. *Chem. Rev.* **2010**, *110*, 7024−7039. (c) Reece, S. Y.; Hodgkiss, J. M.; Stubbe, J.; Nocera, D. G. *Philos. Trans. R. Soc., B* **2006**, *361*, 1351−1364. (d) Wenger, O. S. *Acc. Chem. Res.* **2013**, *46*, 1517−1526.

(3) (a) Barnett, R. N.; Cleveland, C. L.; Joy, A.; Landman, U.; Schuster, G. B. *Science* **2001**, *294*, 567−571. (b) Marcus, R. A. *J. Phys. Chem. B* **1998**, *102*, 10071−10077. (c) Abraham, B.; McMasters, S.; Mullan, M. A.; Kelly, L. A. *J. Am. Chem. Soc.* **2004**, *126*, 4293−4300. (d) Rosokha, S. V.; Sun, D.; Fisher, J.; Kochi, J. K. *ChemPhysChem* **2008**, *9*, 2406−2413. (e) Gao, J.; Müller, P.; Wang, M.; Eckhardt, S.; Lauz, M.; Fromm, K. M.; Giese, B. *Angew. Chem., Int. Ed.* **2011**, *50*, 1926−1930. (f) Yasutomi, S.; Morita, T.; Kimura, S. *J. Am. Chem. Soc.* **2005**, *127*, 14564−14565. (g) Fukuzumi, S.; Ohkubo, K.; D'Souza, F.; Sessler, J. L. *Chem. Commun.* **2012**, *48*, 9801−9815. (h) Park, J. S.; Karnas, E.; Ohkubo, K.; Chen, P.; Kadish, K. M.; Fukuzumi, S.; Bielawski, C. W.; Hudnall, T. W.; Lynch, V. M.; Sessler, J. L. *Science* **2010**, *329*, 1324−1327.

(4) Bhosale, R.; Sakai, N.; Mísek, J.; Matile, S. *Chem. Soc. Rev.* **2010**, *39*, 138−149.

(5) (a) Sakai, N.; Matile, S. *J. Am. Chem. Soc.* **2011**, *133*, 18542−18545. (b) Areephong, J.; Orentas, E.; Sakai, N.; Matile, S. *Chem. Commun.* **2012**, *48*, 10618−10620. (c) Sforazzini, G.; Turdean, R.; Sakai, N.; Matile, S. *Chem. Sci.* **2013**, *4*, 1847−1851. (d) Sforazzini, G.; Sakai, N.; Orentas, E.; Bolag, A.; Matile, S. *J. Am. Chem. Soc.* **2013**, *135*, 12082−12090.

(6) (a) Bang, E.-K.; Gasparini, G.; Molinard, G.; Roux, A.; Sakai, N.; Matile, S. *J. Am. Chem. Soc.* **2013**, *135*, 2088−2091. (b) Orentas, E.; Lista, M.; Lin, N.-T.; Sakai, N.; Matile, S. *Nat. Chem.* **2012**, *4*, 746−750. (c) Bang, E.-K.; Lista, M.; Sforazzini, G.; Sakai, N.; Matile, S. *Chem. Sci.* **2012**, *3*, 1752−1763.

(7) Charbonnaz, P.; Sakai, N.; Matile, S. *Chem. Sci.* **2012**, *3*, 1492−1496.

(8) Sakai, N.; Mareda, J.; Vauthey, E.; Matile, S. *Chem. Commun.* **2010**, *46*, 4225−4237.

(9) Sakai, N.; Lista, M.; Kel, O.; Sakurai, S.-I.; Emery, D.; Mareda, J.; Vauthey, E.; Matile, S. *J. Am. Chem. Soc.* **2011**, *133*, 15224−15227.

(10) Vauthey, E. *ChemPhysChem* **2012**, *13*, 2001−2011.

(11) Fin, A.; Petkova, I.; Alonso Doval, D.; Sakai, N.; Vauthey, E.; Matile, S. *Org. Biomol. Chem.* **2011**, *9*, 8246−8252.

(12) Hinsberg, W.; Houle, F. A.; Lee, S. W.; Ito, H.; Kanazawa, K. *Macromolecules* **2005**, *38*, 1882−1898.

(13) (a) Myer, Y. P. *Macromolecules* **1969**, *2*, 624−628. (b) Zimmermann, R.; Kratzmüller, T.; Erickson, D.; Li, D.; Braun, H.-G.; Werner, C. *Langmuir* **2004**, *20*, 2369−2374. (c) Baumeister, B.; Som, A.; Das, G.; Sakai, N.; Vilbois, F.; Gerard, D.; Shahi, S. P.; Matile, S. *Helv. Chim. Acta* **2002**, *85*, 2740−2753.

(14) Coropceanu, V.; Cornil, J.; da Silva Filho, D. A.; Olivier, Y.; Silbey, R.; Bredas, J.-L. *Chem. Rev.* **2007**, *107*, 926−952.

(15) Wasielewski, M. R.; Conron, S. M. M.; Thazhathveetil, A. K.; Burin, A. L.; Lewis, F. D. *J. Am. Chem. Soc.* **2010**, *132*, 14388−14390.

(16) Arikuma, Y.; Nakayama, H.; Morita, T.; Kimura, S. *Angew. Chem., Int. Ed.* **2010**, *49*, 1800−1804.

(17) (a) Kim, B. J.; Yu, H.; Oh, J. H.; Kang, M. S.; Cho, J. H. *J. Phys. Chem. C* **2013**, *117*, 10743−10749. (b) Podzorov, V.; Menard, E.; Borissov, A.; Kiryukhin, V.; Rogers, J. A.; Gershenson, M. E. *Phys. Rev. Lett.* **2004**, *93*, 086602.

(18) (a) Fabiano, S.; Yoshida, H.; Chen, Z.; Facchetti, A.; Loi, M. A. *ACS Appl. Mater. Interfaces* **2013**, *5*, 4417−4422. (b) Riedel, I.; Parisi, J.; Dyakonov, V.; Lutsen, L.; Vanderzande, D.; Hummelen, J. C. *Adv. Funct. Mater.* **2004**, *14*, 38−44.

(19) Katz, H.; Lovinger, A.; Johnson, J.; Kloc, C.; Siegrist, T.; Li, W.; Lin, Y.; Dodabalapur, A. *Nature* **2000**, *404*, 478−481.

(20) (a) van der Holst, J. J. M.; van Oost, F. W. A.; Coehoorn, R.; Bobbert, P. A. *Phys. Rev. B* **2009**, *80*, 235202. (b) Pivrikas, A.; Sariciftci, N. S.; Juška, G.; Österbacka, R. *Prog. Photovolt: Res. Appl.* **2007**, *15*, 677−696. (c) Vijila, C.; Singh, S. P.; Williams, E.; Sonar, P.; Pivrikas, A.; Philippa, B.; White, R.; Kumar, E. N.; Sandhya, S. G.; Gorelik, S.; Hobley, J.; Furube, A.; Matsuzaki, H.; Katoh, R. *J. Appl. Phys.* **2013**, *114*, 184503.

(21) (a) Delgado, M. C. R.; Kim, E.-G.; da Silva Filho, D. A.; Bredas, J.-L. *J. Am. Chem. Soc.* **2010**, *132*, 3375−3387. (b) Vura-Weis, J.; Ratner, M. A.; Wasielewski, M. R. *J. Am. Chem. Soc.* **2010**, *132*, 1738−1739.

(22) Singh, T. B.; Erten, S.; Guenes, S.; Zafer, C.; Turkmen, G.; Kuban, B.; Teoman, Y.; Sariciftci, N. S.; Icli, S. *Org. Electron.* **2006**, *7*, 480−489.

(23) Giese, B.; Eckhardt, S. *Chimia* **2013**, *67*, 200−203.